

# Low bandgap polymers for photon harvesting in bulk heterojunction solar cells

Christoph Winder and Niyazi Serdar Sariciftci

Christian Doppler Laboratory for Plastic Solar Cells, Linz Institute for Organic Solar Cells (LIOS), Physical Chemistry, Altenbergerstrasse 69, Johannes Kepler University Linz, 4040 Linz, Austria

Received 11th June 2003, Accepted 5th January 2004  
First published as an Advance Article on the web 19th February 2004

Encouraging progress has been made over the last few years in the field of photovoltaic solar cells using organic materials. Among the different concepts which have been proposed, the bulk heterojunction approach (formed by blending donor type conjugated polymers and acceptors like fullerenes) is attractive and significant progress in improving the power conversion efficiency of these devices was obtained recently. One of the possible improvements of this type of solar cells is the implementation of new materials absorbing the red and near infrared part of the solar spectrum, where the maximal photon flux of the sun is located. In this article, we will describe this strategy of photon harvesting in organic solar cells and review recent advances in the search for new materials as candidates for polymeric absorbers.

## 1. Introduction

### 1.1. Organic and polymeric solar cell devices

Organic materials have gained broader interest for implementation in photovoltaic solar cells in the last few years.<sup>1–4</sup> Since the report of a molecular thin film organic solar cell by Tang,<sup>1</sup> several concepts have been presented using small molecules,<sup>1,2</sup> conjugated polymers,<sup>5</sup> conjugated polymer blends,<sup>4,6,7</sup> polymer–small molecule bilayers<sup>8,9</sup> and blends<sup>3,10,11</sup> or combinations of

organic–inorganic materials.<sup>12,13</sup> Organic materials have several advantages such as low cost synthesis and comparatively easy manufacture of thin film devices by vacuum evaporation or solution cast technologies. Furthermore, organic thin films may show optical absorption coefficients<sup>14</sup> exceeding  $10^5 \text{ cm}^{-1}$ , which makes them good chromophores for optoelectronic applications. Among these materials, conjugated polymers are of special interest for several reasons:

- (i) The possibility of an all polymer device (plastic solar cell).
- (ii) The possibility of using solution cast processes such as spin coating or doctor blade<sup>15</sup> or screen-printing<sup>16</sup> for thin film fabrication.
- (iii) Solution cast processes offer an easy way of forming blends of materials, *i.e.* bulk heterojunction devices by processing from common solutions.

### 1.2. Photoinduced charge separation

Unlike the situation in inorganic materials, primary photo-excitations in organic materials do not directly lead to free charge carriers in general, but to coulombically bound electron–hole pairs, called excitons. The nature of these excitons in conjugated polymers has been discussed at length in the scientific community over the last few years.<sup>17</sup> In particular, the magnitude of the exciton binding energy (*i.e.* weakly bound Wannier type excitons *versus* strongly bound Frenkel

Christoph Winder studied Technical Chemistry at the Johannes Kepler University of Linz, Austria, and received his masters degree in Physical Chemistry in 2001 in the group of Prof.



Christoph Winder

N. S. Sariciftci. Since then he has been undertaking his PhD thesis at the Christian Doppler Laboratory for Plastic Solar Cells at the Linz Institute for Organic Solar Cells (LIOS) under the mentorship of Prof. Sariciftci. His main research activity is in spectroscopic studies on conjugated polymers and fullerenes and their application in polymer solar cells.

Niyazi Serdar Sariciftci received his masters degree in Experimental Physics and a doctorate degree in Semiconductor

Physics under the mentorship of Prof. H. Kuzmany at the University of Vienna in 1986 and 1989, respectively. After a post doctoral period at Stuttgart University, Germany, with



Niyazi Serdar Sariciftci

Prof. M. Mehring, he joined the Institute of Polymer and Organic Solids at the University of California, Santa Barbara, with Prof. Alan Heeger. He was appointed Chair and Professor in Physical Chemistry at the Johannes Kepler University of Linz in 1996. He is the Founding Director of the Christian Doppler Laboratory for Plastic Solar Cells and the Linz Institute for Organic Solar Cells (LIOS). His main research activities are in organic semiconductor physics and chemistry.

excitons) plays an important role in understanding the nature of the primary photoexcitations.

In conjugated polymers it is estimated that at room temperature approximately 10% of the photoexcitations lead to free charge carriers.<sup>18</sup> All the other excitons decay *via* radiative or non-radiative recombination pathways and their energy is lost for the power conversion. One possibility to break these excitons into charge carriers is the combination of conjugated polymers with an electron acceptor, for example fullerenes.<sup>19</sup> Charge separation by photoexcitation with a high quantum efficiency was demonstrated for various conjugated polymers and fullerenes. The photoinduced charge transfer in these blends happens on an ultrafast timescale of up to 45 femtoseconds, which is much faster than any other competing relaxation process.<sup>20</sup> The separated charges in such blends are in return metastable at low temperatures. Their lifetime at room temperature is sufficiently long (up to milliseconds) to be transported to the electrodes in a thin film photovoltaic device made thereof.

Whereas the linear absorption spectrum of these donor/acceptor blends is at a first approximation the combination of the single component's absorption spectra, the photoinduced charge transfer leads to drastic changes in the excited state.<sup>21</sup>

(i) The photoluminescence of the conjugated polymer is heavily quenched: Conjugated polymers show in general a strong photoluminescence (as well as electroluminescence). In the mixture with fullerenes, the depopulation of the photoexcited state of the conjugated polymer by this photoinduced charge transfer reaction onto the fullerenes is much faster than the radiative decay ( $\tau \sim 500\text{--}800$  ps). Already the addition of 10% w/w fullerene to the polymer is sufficient to quench the luminescence of the conjugated polymer by a factor of  $>100$ .

(ii) Two strong light induced electron spin resonance (LESR) signals are observed due to the radical ions of the photoinduced charge carriers.<sup>19</sup> The signal with  $g = 2.0026$  is assigned to a positive polaron on the conjugated polymer and the  $g = 1.9997$  signal is assigned to the negative fullerene anion.<sup>22</sup> This latter value is unusually low compared to other carbon based organic radical ions and makes fullerene anion radical unambiguously identifiable.

(iii) Two photoinduced absorption bands within the optical gap are observed by pump-probe techniques. These two bands are assigned to the high- (HE) and low energy (LE) absorption of the polaronic state of the conjugated polymer. The formation of this polaronic band happens in a timescale of 45 fs. The stimulated emission, as probe for the excited state, is quenched in a similar time.<sup>20</sup> The signal of the polaronic peaks is observable until the micro- and even millisecond time regime, showing the long lifetime of the photoinduced charges.<sup>23</sup> In the mid infrared regime, photoinduced infrared active vibrations (IRAVs) are observed as a signature of polaronic relaxation of the lattice. Due to the formation of charged polarons, symmetry forbidden  $A_g$  vibrations of the polymer are activated in the IR and thus observed in the photoinduced IR absorption spectra.<sup>24</sup>

(iv) Time resolved transient photocurrent spectroscopy shows strong sensitization of the photoconductivity of the conjugated polymer upon addition of a small percentage of fullerenes.<sup>25</sup> Both, the magnitude and the lifetime of the photocurrent are increased significantly.

These experimental results show undoubtedly the formation of separated and long living charge carriers in, for example, poly(*para*-phenylene-vinylene)s (PPV)-fullerene or polythiophene (PT)-fullerene blends. The quantum efficiency of this process is close to 100% at the donor-acceptor interface. The above listed spectroscopic techniques are probes for photoinduced charge transfer in polymer-acceptor blends and are used routinely for the investigation of new materials and materials combinations.

### 1.3. Photovoltaic device architectures

Bilayer devices of p- and n-type (donor and acceptor, respectively) organic semiconducting materials were realized for many combinations.<sup>1,2,8,9,26,27</sup> The conversion efficiency of such devices is limited by the charge generation at the donor-acceptor interface. In the case of PPV, this interfacial photoactive layer thickness is in the range of 5–10 nm,<sup>27–30</sup> *i.e.* only excitons created within this distance of the interface can reach the heterojunction interface. This leads to the loss of photons absorbed further away from the interface and leads to low quantum efficiencies. Antibatic behaviour of the photocurrent action spectra as compared to the optical absorption spectrum of the active material is observed due to optical filter effects of the absorbing material before the light gets to the interface.<sup>31</sup> Further, the film thickness has to be optimised for interference effects<sup>32,33</sup> *versus* charge transport.

With the invention of the bulk heterojunction,<sup>3,6</sup> blending the donor and acceptor material, the exciton diffusion bottleneck could be overcome and efficient charge generation in the whole volume of the active layer is ensured. For soluble materials, such blends can be easily realized by casting the composite film from a common solution of the donor and acceptor.

The driving force for the transport of the photoinduced charges to the opposite electrodes in such bulk heterojunction solar cells is still unclear. Several concepts have been proposed, attributing the charge transport either to electric field induced drift of charge carriers or concentration gradient induced diffusion of them, respectively.<sup>34</sup>

The metal-insulator-metal picture,<sup>35</sup> introduced by Parker to describe current-voltage curves of polymeric light emitting diodes, attributes the charge transport to an electric field induced drift, induced by the workfunction difference of the electrodes.

The diffusion-limited concept sees the diffusion of charge carriers induced by concentration gradients as the driving force for transport and attributes directionality only to selective electrodes.<sup>36</sup> Common for both concepts is that the charge transport is directed by the asymmetry of the electrodes properties.

Recently, Gregg and Hanna<sup>37</sup> proposed a new model of an excitonic solar cell, describing all types of organic solar cells. The driving force for the charge transport is assigned to the chemical potential gradient, formed by the charge generation at the interface. The charges are moving away from this interface to the opposite electrodes. In contrast to classical inorganic solar cells, the built-in field is not limiting the open circuit potential, but the photoinduced quasi fermi level difference for positive and negative charges.

Fig. 1 shows the device structure, which is typically used today for bulk heterojunction devices. As positive electrode, indium-tin-oxide ITO coated glass or plastic is used. The ITO is further coated with a layer of poly-ethylene-dioxythiophene:polystyrene-sulfonic acid (PEDOT:PSS) blend. PEDOT is a highly p-doped

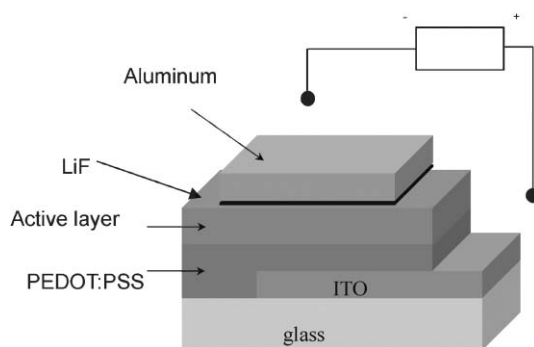


**Fig. 1** Device architecture for a thin film bulk heterojunction photovoltaic device.

water-soluble conjugated polymer, which can be considered as a metal and therefore as the quasi electrode. The PEDOT:PSS layer smooths out the rather rough ITO surface; additionally it influences and increases the work function of the positive electrode. The workfunction of PEDOT:PSS is at  $\sim 5$  eV vs. vacuum, whereas the workfunction of ITO is rather undefined and reported to be between 4.7 and 4.9 eV dependent on the treatment.<sup>38,39</sup> Both materials, the ITO and the PEDOT:PSS used in these devices, are highly transparent in the region between 350 and 900 nm.

The active layer, consisting of the conjugated polymer–fullerene mixture, is coated on top of this electrode. An excess of fullerene is favourable for the percolated transport of the negative charges. So, an optimised polymer to fullerene ratio of 1 : 4 w/w has been reported for [poly(2-methoxy-5-(3,7-dimethyloctyloxy)-*para*-phenylene-vinylene) (MDMO-PPV) and [6,6]-phenyl C<sub>61</sub> butyric acid methylester (PCBM) and 1 : 2 for poly-3-hexylthiophene (P3HT):PCBM, respectively. These two systems show power conversion efficiencies of 2.5% for MDMO-PPV<sup>10,40</sup> and over 3% for P3HT.<sup>41,42</sup>

As top (negative) electrode, a metal layer, such as Al, Ca or Au, is evaporated.<sup>43</sup> An interfacial layer of thermally evaporated LiF was demonstrated to be favourable between the organic and the metal layer in combination with Al and Au.<sup>44</sup> LiF is known to form better electron injecting/collecting contacts with organic thin films in LED devices.<sup>45,46</sup>

#### 1.4. Improving the solar cell device efficiency

The photovoltaic power conversion efficiency  $\eta_e$  is defined by eqn. (1).

$$\eta_e = \frac{V_{OC} * I_{SC} * FF}{P_{in}} \quad (1)$$

$$FF = \frac{I_{mpp} * V_{mpp}}{V_{OC} * I_{SC}} \quad (2)$$

where  $V_{OC}$  is the open circuit voltage,  $I_{SC}$  is the short circuit current, FF is the fill factor, defined in eqn. (2) and  $P_{in}$  the incident light power, which is standardized at  $1000 \text{ W m}^{-2}$  for solar cell testing with a spectral intensity distribution matching that of the sun on the earth's surface at an incident angle of  $45^\circ$ , which is called the AM 1.5 spectrum.  $I_{mpp}$  and  $V_{mpp}$  are the current and voltage at the maximum power point in the fourth quadrant of the current–voltage characteristics. For testing in the laboratory, solar simulators are used to imitate AM 1.5 solar irradiation.

We shall now discuss the critical cell parameters in detail.

**1.4.1. Open circuit voltage.** The thermodynamic limit for the  $V_{OC}$  is given by the bandgap of the active materials. The bandgap limits the splitting of the quasi fermi level of electron and hole, induced by the light absorption. For organic heterojunction devices, instead of the bandgap the energetic distance between the HOMO of the donor and the LUMO of the acceptor has to be considered as the limitation for the  $V_{OC}$ . For bulk heterojunction devices containing a fullerene derivative used, but only weakly dependent on the metal workfunction used as the negative electrode.<sup>43</sup> In contrast to this, Ramsdale *et al.*<sup>47</sup> observed a linear relation of the negative electrode workfunction and the observed open circuit voltage for donor–acceptor polyfluorene bilayer devices. An additional contribution of 1 V to the workfunction difference of the electrodes was observed, which is attributed to the photo-induced dipole formed at the interface due to the charge transfer.

For the positive contact, where ITO coated with PEDOT:PSS is regularly used, a strong dependence of the open

circuit voltage on the work function of the PEDOT:PSS electrode<sup>48</sup> was demonstrated. Lee *et al.* also observed a linear dependence of the open circuit voltage on the HOMO level of the polymeric donor used in bulk-heterojunctions.<sup>49</sup>

**1.4.2. Short circuit current.** The  $I_{SC}$  is determined by the amount of absorbed light and the internal conversion efficiency. An experimentally accessible value is the external quantum efficiency or incident photon to current efficiency, IPCE [%], defined and calculated using eqn. (3).

$$IPCE = \frac{\#_{EI}}{\#_{Ph}} = \frac{1240 * I_{SC}}{\lambda * P_{In}} \quad (3)$$

where  $\lambda$  [nm] is the incident photon wavelength,  $I_{SC}$  [ $\mu\text{A cm}^{-2}$ ] is the photocurrent of the device and  $P_{In}$  [ $\text{W m}^{-2}$ ] is the incident power. IPCE values up to 76% at the absorption maximum are reported for bulk heterojunction solar cells.<sup>10,40–42</sup> The internal quantum efficiency, the ratio of external current to absorbed photons, is estimated to be close to 100% for conjugated polymer–fullerene blends. For an increase in the photocurrent, the light absorption has to be increased. Increasing the thickness is limited due to the low mobility of the charges and possible recombination losses.

The absorption profile of the active layer shows a strong mismatch to the solar photon flux, as compared in Fig. 2. In order to get more efficient devices, materials absorbing in the maximum of the solar photon flux, between 600 and 800 nm, are desirable. The search and development of such materials is one of the important topics for polymer bulk heterojunction solar cells. Recent advances in this search will be reviewed in this article.

**1.4.3. Fill factor (FF).** The FF is defined by eqn. (2) and describes the quality of the diode. The fill factor is mainly influenced by the series and shunt resistances, see the simplified equivalent circuit for a photovoltaic device in Fig. 3.

The nanomorphology of donor/acceptor composites is known to have an important influence on device efficiency.<sup>50</sup> A large interface between the donor/acceptor phases is desired for efficient charge separation. Several approaches have been suggested in the literature to control or manipulate the morphology:

- “Double cables” are materials which consist of a conjugated polymer backbone with acceptor molecules covalently attached. The double cables can be seen as a molecular heterojunction.<sup>51</sup> This approach has been recently reviewed by Cravino *et al.* in this journal.<sup>52</sup>
- Another material structure are block copolymers with alternating conjugated donor and fullerene bearing blocks.<sup>53</sup> It

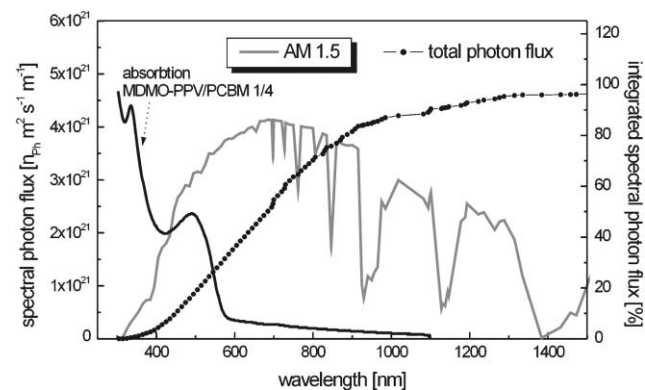


**Fig. 2** AM 1.5 spectrum, defined as the spectral photon flux on the earth's surface under illumination of  $45^\circ$ , in comparison with the absorption profile of a MDMO-PPV : PCBM (1 : 4) film. Circles show the total photon flux, *i.e.* percentage of photons available for a material with a certain bandgap.

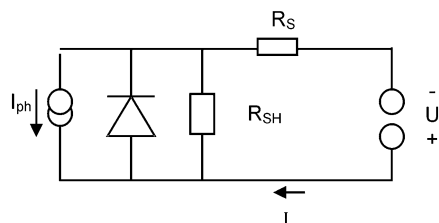


**Fig. 3** Equivalent circuit for a single junction solar cell. The photogenerated current  $I_{ph}$  shows in the inverse direction of the forward one of the diode. Shunt resistance  $R_{SH}$  and series resistance  $R_S$  are important for the fill factor. Ideally, the series resistance should be low and the shunt resistance high.

was shown that these materials are able to form supramolecular self-assemblies.<sup>54</sup>

- The composite nanomorphology can be influenced by changing the conditions during film formation. A dramatic influence of the solvent used was observed on the nanomorphology of devices and, in consequence, device performance.<sup>10,55,56</sup>

- Diffusion bilayers were demonstrated, formed by either lamination of a donor-rich and an acceptor-rich layer<sup>4</sup> or by temperature induced diffusion of an acceptor molecule into the donor polymer matrix.<sup>57</sup>

- Jenekhe *et al.* demonstrated the formation of encapsulated fullerene nanoparticles.<sup>58</sup>

- Recently, Kietzke *et al.* showed the formation of nanospheres by a miniemulsion process to control phase separation with applicability for photovoltaic devices.<sup>59</sup>

## 2. Bandgap tuning of conjugated polymers

The existence of a bandgap for a one-dimensional system, which conjugated chains are, was already predicted by Peierls<sup>60</sup> in 1956, long before the first synthesis of a polyacetylene was reported by Shirakawa in 1971. Peierls predicted in his theorem the lifting of the bond length degeneracy, leading to significant bond length alternation, which causes the bandgap in one-dimensional systems. In the case of polyacetylene it is around 1.4 eV. The intrinsic bandgap of conjugated polymers is generally ascribed to four contributions related to the conjugated polymer backbone,<sup>61,62</sup> shown in Fig. 4a. Additional, intermolecular interactions can further influence the bandgap in the solid state. The individual factors and their impact on the synthesis of low bandgap polymers will be presented in the following discussion.

### 2.1. Bond length alternation ( $E_I$ )

The origin of a Peierls gap is directly related to the bond length alternation. Fig. 4b shows the potential energy as a function of the bond length alternation, which shows two distinct minima. In the case of conjugated polymers with a non-degenerate ground state, like most polyaromatic conjugated polymers are, these two minima have different energy values and are assigned to an aromatic and a quinoid form, see the lower part of Fig. 4b.

Manipulating the bond length alternation was shown to be a powerful tool to manipulate the bandgap. For example, polyisothianaphthenes<sup>63–65</sup> show a bandgap of 1.0 eV, compared to 2.0 eV for polythiophenes. This change is assigned to the increased contribution of the quinoid form of the thiophene ground state,<sup>66</sup> induced by the aromatic benzene ring condensed to the thiophene.

### 2.2. Aromaticity (RE)

Most conjugated polymers have aromatic units as monomers; the aromaticity is preserved in the polymer structure. The aromaticity energy is defined as the energy difference between

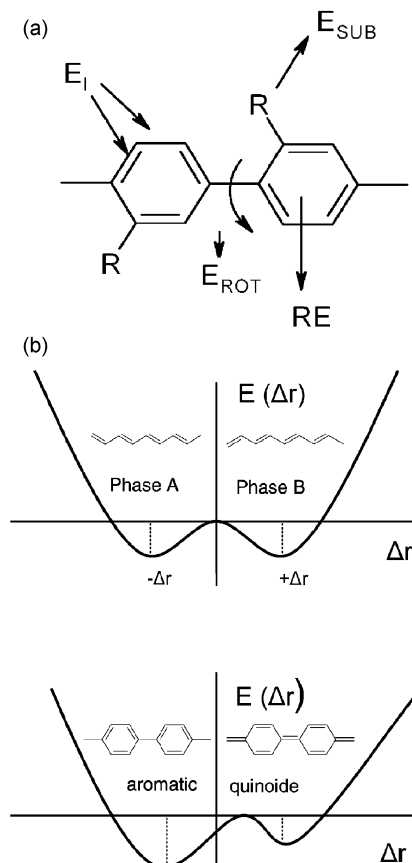


**Fig. 4** (a) Influences of the chemical structure and conformation on the bandgap of the conjugated polymer, here for example poly-*para*-phenylene PPP. (b) Potential energy as a function of bond length alternation, in the upper picture for a conjugated polymer with degenerate groundstate, for example *trans*-polyacetylene, the lower picture shows the potential energy for a conjugated polymer with non-degenerate groundstate, in the given example PPP.

the aromatic structure and a hypothetical reference, consisting of isolated double bonds. Aromaticity leads to a confinement of the  $\pi$ -electron on the ring and competes with the delocalisation.

### 2.3. Conjugation length ( $E_{ROT}$ )

The longer the conjugation on the backbone, the smaller the bandgap. It was generally found that the bandgap decreases with increasing conjugation length, approaching a finite value for infinite conjugation length. Torsion between the adjacent rings partially interrupts the conjugation and leads to an effective increase of the bandgap.

### 2.4. Substituent effects ( $E_{SUB}$ )

Substituents can change the energetic position of the HOMO or LUMO level, respectively, *via* mesomeric or inductive effects. Electron donating groups raise the energetic position of the HOMO. Electron withdrawing groups lower the energetic position of the LUMO.

### 2.5. Intermolecular interactions

Conjugated polymers in the solid state generally show a lower bandgap as compared to the solution phase, which is attributed to an increased interaction between the chains. Furthermore, mesoscopically ordered phases of conjugated polymers could occur, which show a significant decrease of the bandgap as compared to the disordered phases.

Furthermore, bulky side chains can hinder intermolecular interactions between the backbones. Also, much influence has been observed by the regio-stereochemistry of the sidegroups.

As example, regioregularly substituted poly-3-alkylthiophene show, in general, a lower bandgap compared to their regiorandom counterparts.<sup>67,68</sup>

Different structure elements have been proposed to influence the bandgap of conjugated polymers. For example, two widely used approaches are:

- Push-pull polymers with alternating electron rich and electron poor units.
- The introduction of a methine group between the rings is a further popular way to decrease the bandgap. By this approach, the double bond character of the bridging bond leads to a more flat structure and hinders angular rotation between the rings.

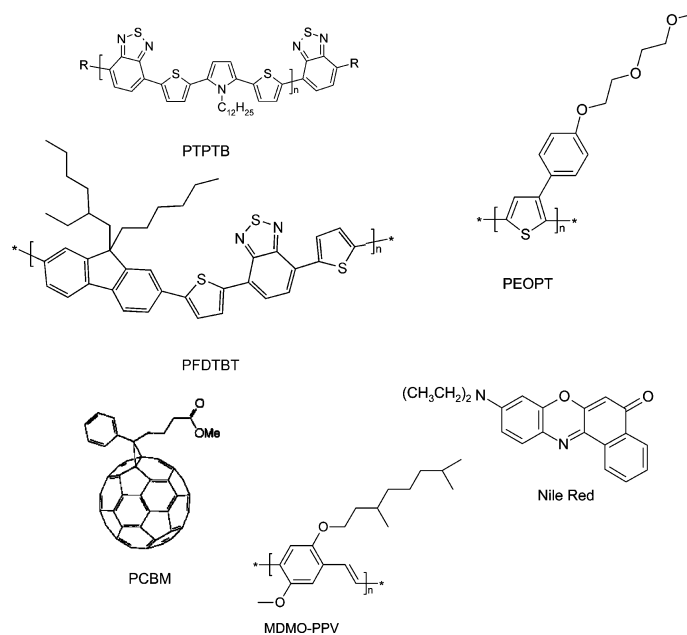
Due to a better theoretical understanding,<sup>60,61,69,70</sup> and much synthetic effort, several new polymers have been proposed with a lower bandgap such as poly-ethylenedioxythiophene,<sup>71</sup> poly-dithienothiophenes<sup>72-74</sup> or copolymers.

Fig. 5 shows the chemical structure of the low bandgap materials discussed in this review, together with MDMO-PPV, the fullerene acceptor PCBM and the dye nile red.

### 3. PEOPT — polythiophenes with a tuneable bandgap

Polythiophenes are a versatile class of conjugated polymers which have been investigated for a wide range of applications.<sup>75</sup> For some 3-alkyl-substituted thiophenes, a thermally activated absorption shift was observed.<sup>76</sup> This shift was attributed to a conformational change of the polymer backbone, induced by a side chain ordering. Longer effective conjugation length by decreased steric hindrance and increased interchain interactions leads to a reduction of the HOMO-LUMO gap. X-Ray diffraction studies on a wide range of phenyl-substituted thiophenes proved the occurrence of ordered crystalline phases in this class of polymers.<sup>77,78</sup> In the absorption, a significant redshift is observed, which is attributed to the occurrence of a crystalline phase. The recently discovered postproduction treatment in bulk heterojunction photovoltaic devices using poly-3-hexylthiophene is partially explained by these effects.<sup>42</sup>

The regioregular poly(3-(4-(1'',4'',7''-trioxaocetyl)phenyl)thiophene) PEOPT<sup>78-80</sup> (Fig. 5) shows the specific case that



**Fig. 5** Chemical structures of the materials discussed in the text: poly *N*-dodecyl-2,5-bis(2-thienyl)pyrrol(2,1,3-benzothiadiazole) (PTPTB), copolymer poly(2,7-(9-(2'-ethylhexyl)-9-hexyl-fluorene)-*alt*-5,5-(4',7'-di-2-thienyl-2',1',3'-benzothiadiazole)) (PFDTBT), poly(3-(4-(1'',4'',7''-trioxaocetyl)phenyl)thiophene) (PEOPT); [6,6]phenyl C<sub>61</sub> butyric acid methyl ester (PCBM) and 9-(diethylamino)-5*H*-benzo[*a*]phenoxazin-5-one (nile red), poly(2-methoxy-5-(3,7-dimethyloctyloxy)*para*-phenylene-vinylene) (MDMO-PPV).

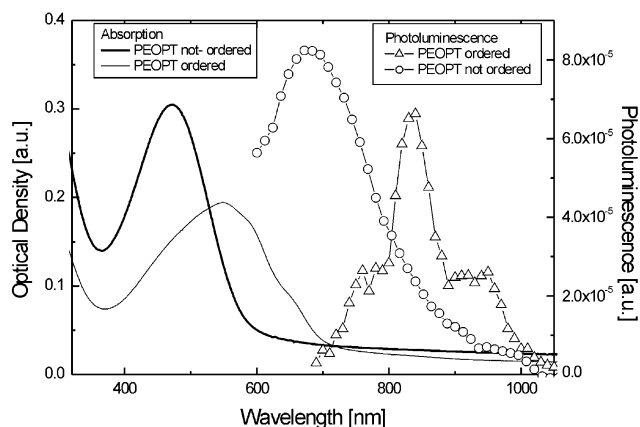


**Fig. 6** Optical absorption and photoluminescence of PEOPT films in the non-ordered and ordered form. The photoluminescence is measured at 100 K with excitation at 488 nm.

both the non-crystalline and partially crystalline phases are metastable and that the non-crystalline phase can be transferred into the partially crystalline one easily. This shift can be seen by eye due to the colour change from orange to blue by transforming from the non-ordered to the ordered phase. The bandgap is changed from the non-ordered to the ordered phase from 2.1 to 1.75 eV, see Fig. 6 for the absorption and emission spectrum. The non-ordered form shows a single absorption peak, whereas the ordered form shows several shoulders to the low energy end, which are typical vibronic satellites for crystalline phases in conjugated polymers.<sup>66</sup> The photoluminescence is shifted for the different phases coincidentally with the absorption. Interestingly, a strong solvatochromism can be observed. The absorption spectra in good solvents like chloroform resemble the orange phase, whereas the absorption spectrum in benzene shows shoulders to the low energy end, typical for the ordered phase.

The same two phases seen for PEOPT are also observed in blends with PCBM. The orange phase is obtained by spin casting from chloroform. This can be transferred to the blue phase by heat treatment at 100 °C for ten minutes or by treatment with chloroform vapour. Furthermore, the blue phase is

obtained by spin casting from solvents such as chlorobenzene or toluene. Drop casting generally leads to the blue phase.<sup>81</sup>

This change in the nanoscopic order of the polymer shows corresponding changes in the photophysics and the interaction of the excited state with fullerene. Fig. 7a shows the photoinduced absorption spectra of the pristine material in the ordered and non-ordered phase, Fig. 7b the corresponding spectra in blends with the fullerene acceptor PCBM. The non-ordered material shows spectra similar to those observed for many conjugated polymers.

In the pristine material, a single excited state absorption peak is observed below the bandgap, which is generally assigned to a triplet-triplet absorption.<sup>82</sup> This peak is quenched in the mixture with fullerene and two new absorption transitions are observed, which are assigned to the polaronic state absorptions of the polymer cation.

The photoinduced absorption spectra of the ordered form is much more complicated. In the pristine material, see spectra 7a, a complicated pattern with peaks at 1.5, 1.2 and 0.9 eV is observed. By addition of fullerene acceptor, for the PIA spectra see Fig. 7b, the low energy peak at 0.9 eV is quenched, a new peak arising below 0.6 eV. In the blend with PCBM, all transitions are assigned to polaronic absorption. The splitting of the high energy polaron peak was attributed to the existence of two-dimensional delocalised<sup>83</sup> charged photoexcitations.

Recent calculations by Beljonne *et al.*<sup>84</sup> showed interacting chains may give rise to splitting of the polaronic levels. Fig. 8 shows a schematic figure for the one-excitation levels for a polaron on a single chain and for a polaron with cofacial interaction with an adjacent chain. This splitting, which will be heavily dependent on the interchain coupling of the polarons, is presumably much stronger in the ordered phase of the PEOPT and thus can explain this observed splitting in the high energy photoinduced absorption band (see Fig. 7b). We specifically

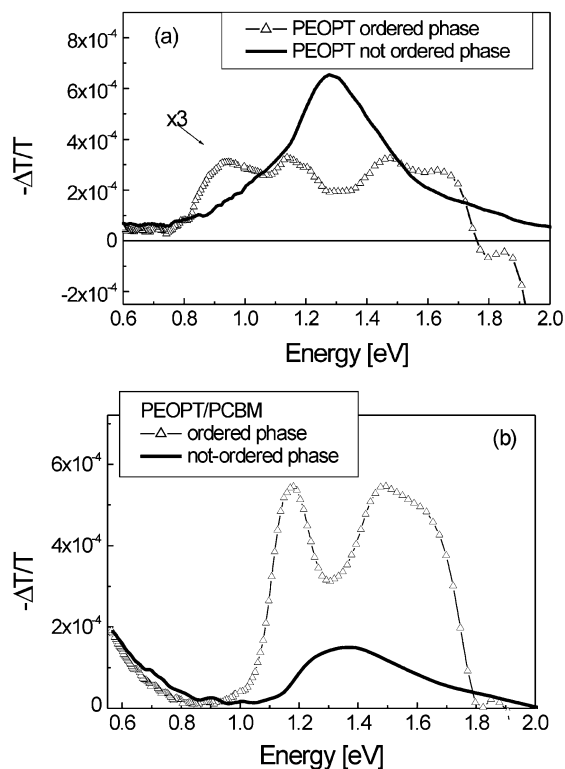


**Fig. 7** (a) Photoinduced absorption spectra of PEOPT in the non-ordered and ordered phase; (b) Photoinduced absorption spectra of PEOPT : PCBM (1 : 1) blends with the polymer in the ordered and non-ordered phase. Spectra were recorded at 100 K with excitation at 488 nm. (Reproduced with permission from the American Institute of Physics from ref. 70).

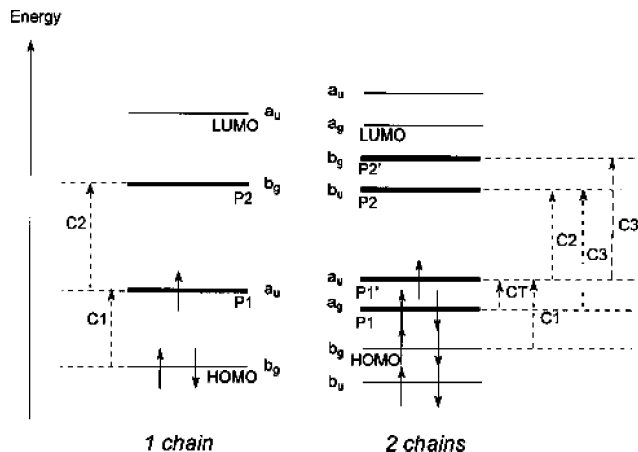
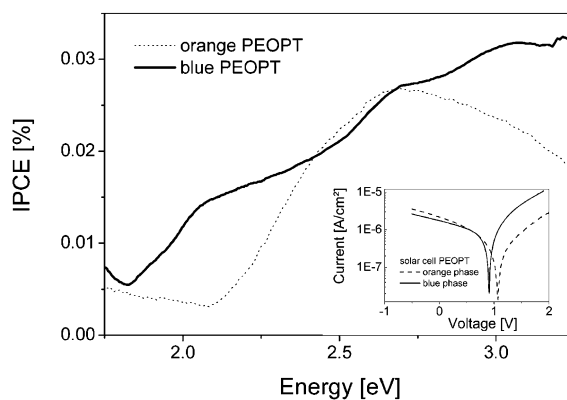


**Fig. 8** Schematic representation of the one electron energy diagram for a polaron localized on a single conjugated chain (left) and delocalised over two cofacial chains (right). The symmetry and the relevant electronic excitation are indicated. (Reproduced with permission of WILEY-VCH from ref. 74).

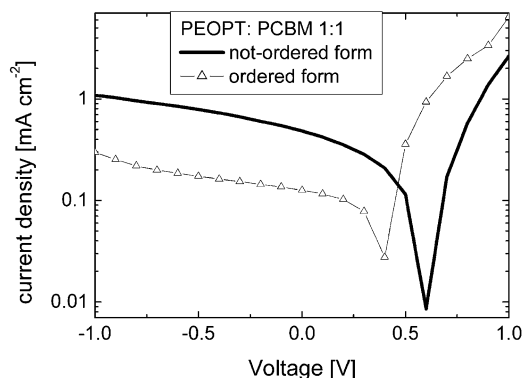
compare our experimental Fig. 7b using the mixtures with the theory of Beljonne *et al.*, calculated for charged polarons, since the efficient photoinduced electron transfer results in charged polarons on the polymer backbone in the blends with fullerenes.

Fig. 9 shows the photocurrent action spectra of photovoltaic devices of PEOPT in its two forms. The spectra of the ordered form are extended to the red as compared to the disordered form, confirming the lower bandgap of the ordered form.

As shown by the photoinduced absorption experiments, interaction of the photoexcited PEOPT with PCBM leads to efficient charge creation. Photovoltaic devices of PEOPT with fullerene acceptor have been demonstrated in bilayer with C<sub>60</sub> as evaporated acceptor layer as well as for bulk heterojunction blends with PCBM. The photocurrent of both forms can be significantly enhanced forming bilayer devices with C<sub>60</sub>.<sup>85</sup> Blending of the two distinct forms of PEOPT with PCBM fullerene acceptor in bulk heterojunction type photovoltaic devices resulted in solar cells with short circuit responses up to 0.5 mA cm<sup>-2</sup> (see Fig. 10). In the ordered phase of PEOPT, however, the quality of the films were poor and the devices lost both in short circuit current and open circuit voltage as compared to the non-ordered phase.



**Fig. 9** Photocurrent spectra of a photovoltaic cell of pristine PEOPT in the non-ordered (orange) and ordered (blue) form. Inset shows the *I*-*V* curve under illumination from a Steuernagel solar simulator. The following values were measured: ordered phase  $V_{OC} = 0.91$  V,  $I_{SC} = 1.9 \mu\text{A cm}^{-2}$ , FF = 0.30; non-ordered phase  $V_{OC} = 1.06$  V,  $I_{SC} = 2.2 \mu\text{A cm}^{-2}$  and FF = 0.24. (Reproduced with permission from the American Institute of Physics from ref. 70).



**Fig. 10** Current–voltage curve of PEOPT : PCBM (1 : 1) diodes with the polymer in the ordered and non-ordered form, under illumination from a solar simulator. For the non-ordered polymer,  $V_{OC} = 0.62$  V,  $I_{SC} = 0.480$   $\mu\text{A cm}^{-2}$  and  $FF = 0.28$ , giving  $\eta = 0.1\%$ ; for the ordered polymer,  $V_{OC} = 0.38$  V,  $I_{SC} = 125$   $\mu\text{A cm}^{-2}$  and  $FF = 0.49$ , giving  $\eta = 0.02\%$ ; films were spin cast from chloroform, top contact Al without LiF.

#### 4. Polyfluorene copolymers

Polyfluorenes are widely used and investigated due to their high mobility and good environmental stability.<sup>86</sup> Furthermore, polyfluorenes show good chemical tunability and can be tailored for the desired optoelectronic properties.<sup>87</sup>

Polyfluorene–benzothiadiazole-copolymers show electron accepting properties<sup>88</sup> and are used for polymer-donor/polymer-acceptor bulk-heterojunction photovoltaic devices.<sup>47</sup> But the photovoltaic power conversion efficiency is limited due to the high bandgap of polyfluorene, which is typically  $\sim 2.4$  eV and even higher than for most PPV derivatives.

Svensson *et al.* recently introduced a new fluorene based copolymer poly(2,7-(9-(2'-ethylhexyl)-9-hexyl-fluorene)-*alt*-5,5-(4',7'-di-2-thienyl-2',1',3'-benzothiadiazole)) PFDTBT,<sup>89</sup> (see Fig. 5). This material shows a red-shifted absorption with an onset around 650 nm as compared to simple polyfluorenes, which have a typical absorption onset around  $< 550$  nm. Devices with PFDTBT/PCBM blend in a ratio of 1 : 4 show power conversion efficiencies of 2.2% ( $V_{OC} = 1.04$  V,  $I_{SC} = 4.66$   $\text{mA cm}^{-2}$ ,  $FF = 0.46$ ,  $P_{in} = 100$   $\text{mW cm}^{-2}$ ). The external quantum efficiency is around 40% at the maximum, which is comparable to MDMO-PPV/PCBM based devices. Interesting is the high open circuit voltage of more than 1 V.

#### 5. PTPTB — a novel low bandgap polymer

PTPTB, consisting of alternating electron-rich *N*-dodecyl-2,5-bis(2'-thienyl)pyrrole (TPT) and electron-deficient 2,1,3-benzothiadiazole (B) units, for the chemical structure see Fig. 5, was synthesised for application as an electron donor polymer in bulk heterojunction solar cells.<sup>90,91</sup> The material shows an optical bandgap of 1.7 eV, which is in good agreement with the value determined by electrochemical voltage spectroscopy of 1.8 eV.<sup>92</sup> The onset of the oxidation was determined as  $+0.54$  V vs.  $\text{Ag}/\text{Ag}^+$ . Spectroscopic investigation of blends of PTPTB with fullerene acceptor PCBM demonstrates photoinduced charge transfer between the materials by photoluminescence quenching and the occurrence of polaronic transitions in the blend due to photoexcited charges on the polymer backbone.<sup>91,93</sup> The photocurrent spectrum, in comparison with the optical absorption of a photovoltaic device consisting from the same blend, is shown in Fig. 11a. The spectral photocurrent peaks at 600 nm,<sup>94</sup> coinciding with the absorption maximum, and contributions to the IPCE are observed up to 750 nm. Fig. 11b shows the  $I$ – $V$  curves of a bulk heterojunction device from PTPTB/PCBM (1 : 3 wt ratio). In the dark the current–voltage curve shows a rectification ratio of

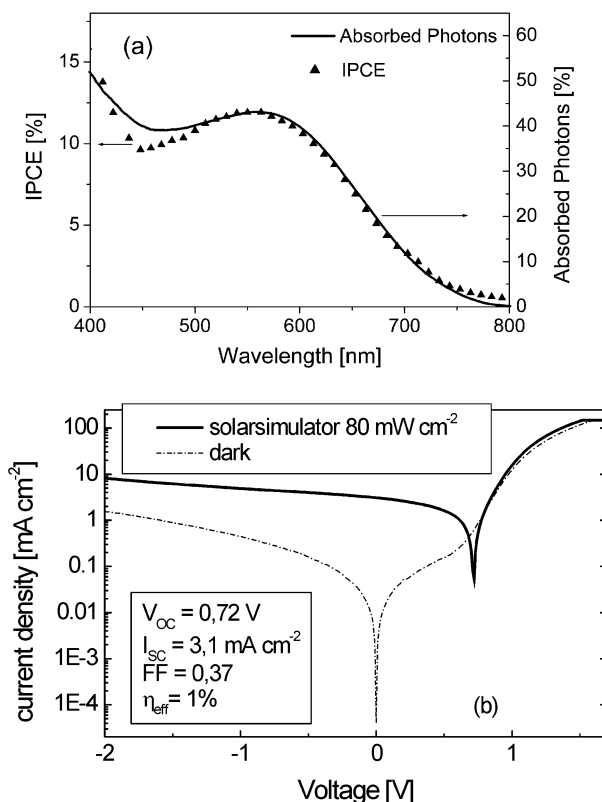


**Fig. 11** (a) Photocurrent spectra IPCE of a photovoltaic device with PTPTB:PCBM (1 : 3) as active layer in comparison with the thin film transmission spectrum. The thickness of the active layer is approximately 100 nm. (b) Current–voltage curve under illumination from a solar simulator with  $80$   $\text{mW cm}^{-2}$  and in the dark from the same device. (Reproduced with permission of WILEY-VCH from ref. 80).

about  $10^2$  at  $\pm 2$  V. Under simulated AM 1.5 illumination, a strong photoeffect is observed. The open circuit voltage of 0.72 V is just 0.1 V less than the highest values observed for MDMO-PPV/fullerene devices although the bandgap of PTPTB is reduced by *ca.* 0.5 eV as compared to MDMO-PPV. The position of the HOMO level of PTPTB is close to that reported for HOMO of MDMO-PPV. Since the energetic position for the positive charge is mainly determined by the HOMO of the donor and the energetic position for the negative charge by the LUMO of the fullerene, this explains the similar values for the open circuit voltage between MDMO-PPV and PTPTB based solar cells. The energetic splitting between the donor HOMO and the acceptor LUMO is the thermodynamic maximum, which can be obtained from this photovoltaic device and can be lowered by several factors, for example low parallel resistance of the device. Instead, the offset between the LUMO levels of the donor and acceptor is lower in the case of PTPTB and PCBM with approximately 0.4 eV instead of MDMO-PPV/PCBM with approximately 1 V. This offset is required for the charge separation, but on the other hand, is also an energetic loss. The short circuit current,  $I_{SC}$ , is measured as  $3$   $\text{mA cm}^{-2}$  and the fill factor  $FF$  is calculated to be 0.37. From these values, the power conversion efficiency  $\eta_{AM1.5}$  is calculated with  $\sim 1\%$ .

While the short circuit current of the device is already high, the overall efficiency of the device is limited by the low fill factor. Generally, low FFs can be induced by high series resistances or by small shunt resistances. For PTPTB/PCBM devices we find serial resistances below  $10$   $\Omega \text{ cm}^{-2}$ , which cannot explain the low FF. Therefore, the low FF is expected to originate from a small parallel shunt resistance in the device. Most likely, the low molecular weight of the polymer, determined as 5–16 aromatic units by size exclusion chromatography, causes the low

film forming quality and the many pinholes that lead to nanoshorts.<sup>95</sup>

## 6. Sensitizing low bandgap polymer — towards carpeting the sun spectrum

By shifting the polymer absorption to the red part of the visible spectrum or even to the near infrared, concurrently the absorption in the blue–green region of the spectrum is lowered. To overcome this problem, an additional component can be added to the blend, for example an organic dye molecule or a wide bandgap conjugated polymer, absorbing in this high energy region. The excited state of this dye ought to make an energy transfer to the lower bandgap polymer, which makes that subsequently the charge transfer reaction. Alternatively, the mechanism of an individual electron transfer by the dye to the fullerene and subsequent hole transfer to the polymer is also possible.

For PTPTB, sensitization with MDMO-PPV and Nile red, for chemical structures see Fig. 5, were investigated. Energy transfer reaction can be monitored by photoluminescence experiments. The low bandgap guest material is dispersed in the wide bandgap host material. After selective excitation of the wide bandgap material, the photoluminescence of the low bandgap material, even at low concentration, is preferentially observed and the photoluminescence of the wide bandgap material is quenched. This could be observed in the case of MDMO-PPV, see Fig. 12a, as well as Nile red in combination

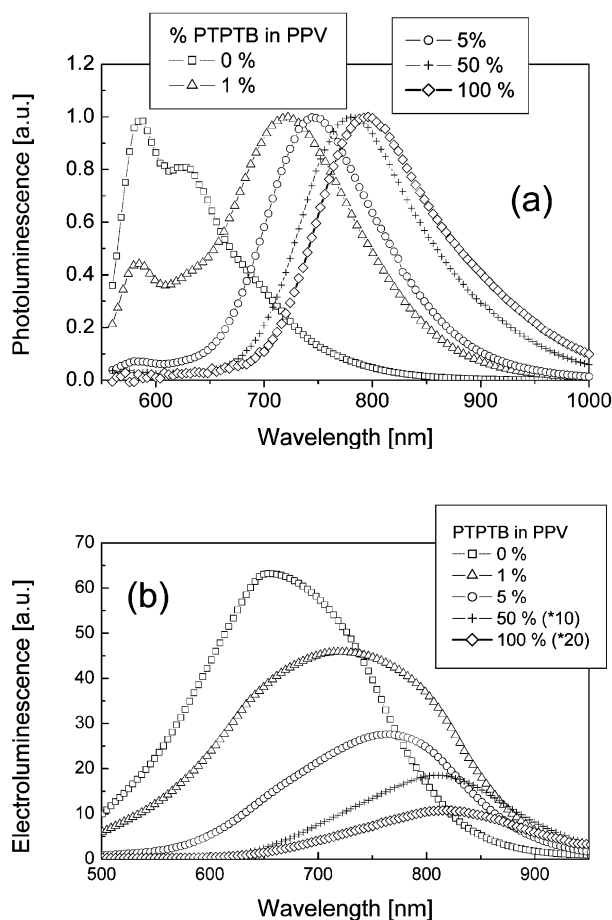


**Fig. 12** (a) Photoluminescence, normalized to the peak maximum, of different MDMO-PPV:PTPTB blends, in comparison to the photoluminescence of pristine materials; excitation at 514 nm is used to excite preferentially MDMO-PPV. (b) Electroluminescence of the corresponding devices with the same active layer. Devices operate at 5 V, or 7 V, in the case of the 50% and pure PTPTB device, respectively. (Reproduced with permission of WILEY-VCH from ref. 74).

with PTPTB.<sup>95</sup> Such host–guest energy transfer systems are widely used in light emitting diodes to sensitize the luminescence of low bandgap materials.<sup>96–98</sup> PTPTB shows electroluminescence in the near infrared region, with a peak around 800 nm. By mixing small amounts of PTPTB into MDMO-PPV, the emission of PTPTB could be increased significantly.<sup>94</sup> The highest emission in the near infrared was observed by blending only 1% w/w of the PTPTB in the MDMO-PPV host, shown in Fig. 12b. Solar cell devices with an active layer consisting of MDMO-PPV:PTPTB:PCBM show efficiencies around 0.5%.<sup>95</sup> Upon blending 10 wt.% of a highly absorbing, dye molecule (Nile red, for the chemical structure see Fig. 5) into the photoactive PTPTB/PCBM blend, no major changes are observed in the dark  $I$ – $V$  characteristics (Fig. 13b). Only the onset for the injection in the forward direction is slightly lowered. Under illumination, the open circuit voltage is found to be reduced from 0.72 to 0.53 V upon addition of the dye. The maximum of the photocurrent is located at 550 nm, coinciding with the absorption maximum of the dye molecule (Fig. 13a). The contribution of PTPTB to the photocurrent is observed in the region between 600 to 750 nm, in this region the photocurrent spectrum is not changed compared to the PTPTB/PCBM device. This device shows the possibility to use combinations of different absorbers to carpet larger ranges of the solar spectrum.

## 7. Concluding remarks and outlook

The efficiency of polymer based bulk heterojunction devices could be steadily increased using several strategies for photon harvesting in organic solar cells:

- Synthesis of new materials with optical absorption at

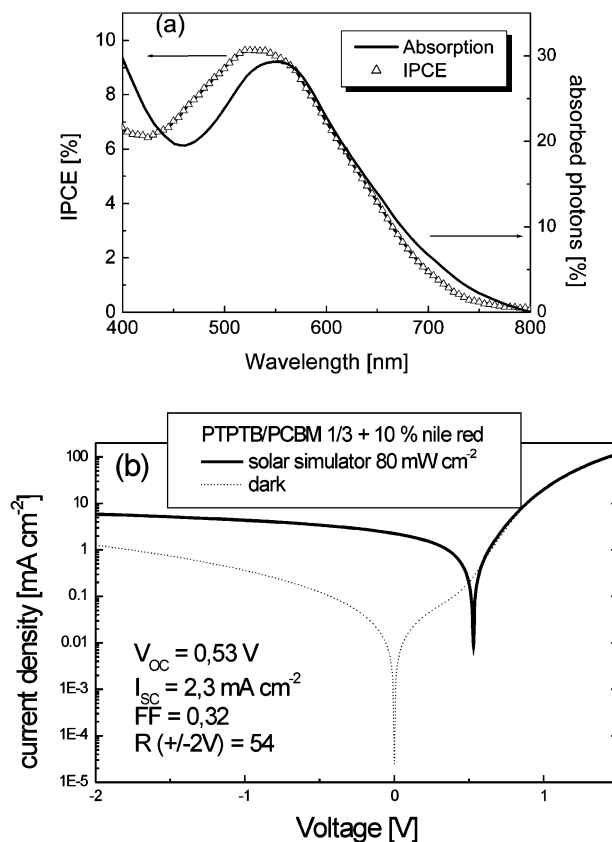


**Fig. 13** (a) Photocurrent spectra IPCE of a photovoltaic device with PTPTB:PCBM (1 : 3) with an additional 10% of the polymer weight Nile red as active layer in comparison with the thin film transmission spectrum. The thickness of the active layer is approximately 100 nm. (b) Current–voltage curve under illumination from a solar simulator with 80 mW cm<sup>-2</sup> and in the dark from the same device.

longer wavelengths. In this article we have reviewed some of the latest developments in the field of low bandgap polymers. Other work has shown the implementation of alternative acceptors to the fullerene, which is not a good absorber in the visible region. Cyano-PPV<sup>4,7</sup> and fluorene-benzothiadiazol copolymer<sup>87</sup> have been demonstrated as acceptor polymers in bilayer and bulk heterojunction devices.

As alternative acceptor molecules, perylene has been widely used as acceptor in combination with small molecule<sup>1,2,99</sup> and conjugated polymers.<sup>9,11,100,101</sup> Recently, the implementation of covalently linked fullerene-dye dyads<sup>102</sup> into organic solar cells was demonstrated.<sup>103,104</sup>

● Energy transfer cascade of different absorbers, carpeting the solar spectrum. An energy transfer cascade is built to transfer the energy from the wide bandgap material to the low bandgap material by energy transfer. Dye-polymer,<sup>94</sup> and polymer-polymer blends have been presented<sup>105</sup> for this purpose.

● Multiple layer solar cells with materials of different bandgaps, similar to the tandem cells for inorganic materials. Serial connection of organic solar cells could be demonstrated by implementing a thin metal layer as tunnelling layer between individual cells.<sup>106,107</sup>

● The use of light scattering nano or micro particles embedded in the optically active layer to enhance the optical pathways in the film due to scattering.

● The use of light trapping mechanisms by structuring the interface of the photovoltaic devices as presented by Niggemann *et al.*<sup>108</sup> and Roman.<sup>109</sup>

● Hybrid solar cells<sup>13,110</sup> are a combination of conjugated polymer donors and inorganic nanoparticle acceptors. Power conversion efficiency of P3HT:CdSe blend devices of 1.7% have been demonstrated for such devices. This approach combines the easy processability of polymer materials with the advantageous absorption profile of inorganic materials. Additionally, the inorganic materials show good transport, which can be optimised by tuning their shape.

● Dye sensitised solar cells, which use organic dyes with absorption onsets around 800 nm on a nanoporous electrode, typically TiO<sub>2</sub>. This approach is widely used in photoelectrochemical cells with an electrolyte as hole conductor. For such cells, power conversion efficiencies of 10% were demonstrated.<sup>12</sup> Recently, an all-solid-state dye sensitized cell, replacing the liquid electrolyte by an organic hole transport layer, with efficiencies of 3.2% was reported.<sup>111</sup>

## 8. Acknowledgements

We thank Rene A. J. Janssen, Mats Andersson and J. Kees Hummelen for providing the materials. Furthermore, we thank Christoph Brabec, Helmut Neugebauer and Dieter Meissner for many fruitful discussions. The work was performed with the Christian Doppler Laboratory for Plastic Solar Cells, financed by Konarka Austria and the Austrian Ministry of Economic Affairs.

## 9. References

- 1 C. W. Tang, *Appl. Phys. Lett.*, 1986, **48**, 183.
- 2 D. Wöhrle and D. Meissner, *Adv. Mater.*, 1991, **3**, 129.
- 3 G. Yu, J. Gao, J. C. Hummelen, F. Wudl and A. J. Heeger, *Science*, 1995, **270**, 1789.
- 4 M. Granström, K. Petritsch, A. C. Arias, A. Lux, M. R. Andersson and R. H. Friend, *Nature*, 1998, **395**, 257.
- 5 H. Antoniadis, B. R. Hsieh, M. A. Abkowitz, S. A. Jenekhe and M. Stolka, *Synth. Met.*, 1994, **62**, 265.
- 6 J. J. M. Halls, C. A. Walsh, N. C. Greenham, E. A. Marseglia, R. H. Friend, S. C. Moratti and A. B. Holmes, *Nature*, 1995, **376**, 498.
- 7 G. Yu and A. J. Heeger, *J. Appl. Phys.*, 1995, **78**, 4510.
- 8 S. A. Jenekhe and S. Yi, *Appl. Phys. Lett.*, 2000, **77**, 2635.

- 9 A. J. Breeze, A. Salomon, D. S. Ginley, B. A. Gregg, H. Tillmann and H. H. Hoerhold, *Appl. Phys. Lett.*, 2002, **81**, 3085.
- 10 S. E. Shaheen, C. J. Brabec, N. S. Sariciftci, F. Padinger, T. Fromherz and J. C. Hummelen, *Appl. Phys. Lett.*, 2001, **78**, 841.
- 11 J. J. Dittmer, E. A. Marseglia and R. H. Friend, *Adv. Mater.*, 2000, **12**, 1270.
- 12 D. O. Reagan and M. Graetzel, *Nature*, 1991, **353**, 737.
- 13 N. C. Greenham, X. Peng and A. P. Alivisatos, *Phys. Rev. B*, 1996, **54**, 17628.
- 14 H. Hoppe, N. S. Sariciftci and D. Meissner, *Mol. Cryst. Liq. Cryst.*, 2002, **385**, 113.
- 15 C. J. Brabec, F. Padinger, J. C. Hummelen, R. A. J. Janssen and N. S. Sariciftci, *Synth. Met.*, 1999, **102**, 861.
- 16 S. E. Shaheen, R. Radspinner, N. Peyghambarian and G. E. Jabbour, *Appl. Phys. Lett.*, 2001, **79**, 2996.
- 17 *Primary Photoexcitations in Conjugated Polymers: Molecular Exciton versus Semiconductor Band Model*, ed. N. S. Sariciftci, World Scientific Publishers, Singapore, 1997.
- 18 P. B. Miranda, D. Moses and A. J. Heeger, *Phys. Rev. B*, 2001, **64**, 81201.
- 19 N. S. Sariciftci, L. Smilowitz, A. J. Heeger and F. Wudl, *Science*, 1992, **258**, 1474.
- 20 C. J. Brabec, G. Zerza, G. Cerullo, S. De-Silvestri, S. Luzatti, J. C. Hummelen and S. Sariciftci, *Chem. Phys. Lett.*, 2001, **340**, 232.
- 21 N. S. Sariciftci and A. J. Heeger, in *Handbook of Organic Conductive Molecules and Polymers*, vol. 1, ed. H. S. Nalwa, Wiley, New York, 1996, pp. 414-450.
- 22 P. M. Allemand, G. Srdanov, A. Koch, K. Khemeni, F. Wudl, Y. Rubin, F. N. Diedrich, M. M. Alvarez, S. J. Anz and R. L. Whetten, *J. Am. Chem. Soc.*, 1991, **113**, 2780.
- 23 A. F. Nogueira, I. Montanari, J. Nelson, J. Durrant, C. Winder, N. S. Sariciftci and C. J. Brabec, *J. Appl. Phys.*, 2003, **107**, 1567.
- 24 E. Ehrenfreund, Z. V. Vardeny, O. Brafman and B. Horowitz, *Phys. Rev. B*, 1987, **36**, 1535.
- 25 C. H. Lee, G. Yu, D. Moses, K. Pakbaz, C. Zhang, N. S. Sariciftci, A. J. Heeger and F. Wudl, *Phys. Rev. B*, 1993, **48**, 15425.
- 26 N. S. Sariciftci, D. Braun, C. Zhang, V. I. Srdanov, A. J. Heeger, G. Stucky and F. Wudl, *Appl. Phys. Lett.*, 1993, **62**, 585.
- 27 J. J. M. Halls, K. Pichler, R. H. Friend, C. S. Moratti and A. B. Holmes, *Appl. Phys. Lett.*, 1996, **68**, 3120.
- 28 T. Stuebinger and W. Bruetting, *J. Appl. Phys.*, 2001, **90**, 3632.
- 29 A. Haugeneder, M. Neges, C. Kallinger, W. Spirkel, U. Lemmer, J. Feldmann, U. Scherf, E. Harth, A. Guegel and K. Muellen, *Phys. Rev. B*, 1999, **59**, 15326.
- 30 M. Theander, A. Yartsev, D. Zigmantas, V. Sundstroem, W. Manno, M. R. Andersson and O. Inganaes, *Phys. Rev. B*, 2000, **61**, 12957.
- 31 M. G. Harrison, J. Gruener and G. C. W. Spencer, *Phys. Rev. B*, 1997, **55**, 7831.
- 32 L. A. A. Pettersson, L. S. Roman and O. Inganaes, *J. Appl. Phys.*, 1999, **86**, 487.
- 33 J. Ronstalski and D. Meissner, *Sol. Energy Mater. Sol. Cells*, 2000, **63**, 37.
- 34 V. Dyakonov, *Physica E (Amsterdam)*, 2002, **14**, 53.
- 35 I. D. Parker, *J. Appl. Phys.*, 1994, **75**, 1656.
- 36 D. Meissner and J. Ronstalski, *Synth. Met.*, 2001, **121**, 1551.
- 37 B. A. Gregg and M. C. Hanna, *J. Appl. Phys.*, 2003, **93**, 3605.
- 38 G. Greczynski, Th. Kugler, M. Keil, W. Osikowicz, M. Fahlman and W. R. Salanck, *J. Electron Spectrosc. Relat. Phenom.*, 2001, **121**, 1.
- 39 J. S. Kim, M. Granstrom, R. H. Friend, N. Johansson, W. R. Salaneck, R. Daik, W. J. Feast and F. Cacialli, *J. Appl. Phys.*, 1998, **84**, 6859.
- 40 C. J. Brabec, N. S. Sariciftci and J. K. Hummelen, *Adv. Funct. Mater.*, 2001, **11**, 15.
- 41 P. Schilinsky, C. Waldauf and C. J. Brabec, *Appl. Phys. Lett.*, 2002, **81**, 3885.
- 42 F. Padinger, R. Rittberger and N. S. Sariciftci, *Adv. Funct. Mater.*, 2003, **13**, 85.
- 43 C. J. Brabec, A. Cravino, D. Meissner, N. S. Sariciftci, T. Fromherz, T. Rispens, L. Sanchez and J. C. Hummelen, *Adv. Funct. Mater.*, 2001, **11**, 374.
- 44 C. J. Brabec, S. E. Shaheen, C. Winder, N. S. Sariciftci and P. Denk, *Appl. Phys. Lett.*, 2002, **80**, 1288.
- 45 L. S. Hung, C. W. Tang and M. G. Mason, *Appl. Phys. Lett.*, 1997, **70**, 151.
- 46 G. E. Jabbour, Y. Kaxabe, S. E. Shaheen, J. F. Wang, M. M. Morrell, B. Kippelen and N. Peyghambarian, *Appl. Phys. Lett.*, 1997, **71**, 1762.

- 47 C. M. Ramsdale, J. A. Barker, A. C. Arias, J. D. MacKenzie, R. H. Friend and N. C. Greenham, *J. Appl. Phys.*, 2002, **92**, 4266.
- 48 H. Frohne, S. Shaheen, C. J. Brabec, D. Mueller, N. S. Sariciftci and K. Meerholz, *Chem. Phys. Chem.*, 2002, **9**, 796.
- 49 H. Kim, S. H. Jin, H. Suh and K. Lee, *Proc. SPIE-Int. Soc. Opt. Eng.*, 2003, in press.
- 50 P. Peumans, S. Uchida and S. Forrest, *Nature*, 2003, **425**, 158.
- 51 A. Cravino and N. S. Sariciftci, *Nature Mater.*, 2003, **2**, 360.
- 52 A. Cravino and N. S. Sariciftci, *J. Mater. Chem.*, 2002, **12**, 1931.
- 53 U. Stalmach, B. de Boer, C. Vidolot, P. F. van Hutten and G. Hadziioannou, *J. Am. Chem. Soc.*, 2000, **122**, 5464.
- 54 B. de Boer, U. Stalmach, P. F. van Hutten, C. Melzer, V. V. Krasnikov and G. Hadziioannou, *Polymer*, 2001, **42**, 9097.
- 55 J. J. M. Halls, A. C. Arias, J. D. MacKenzie, W. Wu, M. Inbasekaran, E. P. Woo and R. H. Friend, *Adv. Mater.*, 2000, **12**, 498.
- 56 A. C. Arias, N. Cocoran, M. Banach, R. H. Friend, J. D. MacKenzie and W. T. S. Huck, *Appl. Phys. Lett.*, 2002, **80**, 1695.
- 57 M. Drees, K. Premaratne, W. Graupner, J. R. Heflin, R. M. Davis, D. Marciu and M. Miller, *Appl. Phys. Lett.*, 2002, **81**, 4607.
- 58 S. A. Jenekhe and X. L. Chen, *Science*, 1998, **279**, 1903.
- 59 T. Kietzke, D. Neher, J. Landfester, R. Montenegro, R. Guenter and U. Scherf, *Nature Mater.*, 2003, **2**, 408.
- 60 R. E. Peierls, *Quantum Theory of Solids*, Oxford University Press, London, 1955.
- 61 J. Roncali, *Chem. Rev.*, 1997, **97**, 173.
- 62 R. Kiesboms, R. Menon and K. Lee, in *Handbook of Advanced Electronic and Photonic Materials and Devices 8*, ed. H. S. Nalwa, Academic Press, San Diego, 2001, pp. 38-47.
- 63 F. Wudl, M. Kobayashi and A. J. Heeger, *J. Org. Chem.*, 1994, **49**, 3382.
- 64 H. Meng and F. Wudl, *Macromolecules*, 2001, **34**, 1810.
- 65 I. Polec, A. Henckens, L. Goris, M. Nicolas, M. A. Loi, P. J. Adriaensens, L. Lutsen, J. V. Manca, D. Vanderzande and N. S. Sariciftci, *J. Polym. Sci., Part A: Polym. Chem.*, 2003, **41**, 1034.
- 66 J. L. Bredas, A. J. Heeger and F. Wudl, *J. Chem. Phys.*, 1986, **85**, 4673.
- 67 R. D. McCullough, R. D. Lowe, M. Jayaraman and D. L. Anderson, *J. Org. Chem.*, 1993, **85**, 904.
- 68 T. D. Chen and R. D. Rieke, *J. Am. Chem. Soc.*, 1998, **8**, 25.
- 69 J. L. Bredas, *Adv. Mater.*, 1995, **7**, 263.
- 70 A. Dkhissi, F. Louwet, L. Groenendaal, B. Beljonne, R. Lazzaroni and J. L. Bredas, *Chem. Phys. Lett.*, 2002, **359**, 466.
- 71 L. B. Groenendaal, F. Jonas, D. Freitag, H. Pielartzik and J. R. Reynolds, *Adv. Mater.*, 2000, **12**, 481.
- 72 C. Arizziani, M. Castellani, C. G. Cerroni and M. Mastagostino, *J. Electroanal. Chem.*, 1997, **423**, 23.
- 73 M. Castellani, R. Lazzaroni, J. L. Bredas and S. Luzzati, *Synth. Met.*, 1999, **101**, 175.
- 74 A. Cravino, H. Neugebauer, S. Luzzati, M. Castellani, A. Petr, L. Dunsch and N. S. Sariciftci, *J. Phys. Chem. B*, 2002, **106**, 3583.
- 75 H. Sirringhaus, N. Tessler and R. H. Friend, *Science*, 1998, **280**, 1741.
- 76 K. Yoshino, S. Nakajima, D.-H. Park and R. Sugimoto, *Jpn. J. Appl. Phys., Part 2*, 1988, **27**, 716.
- 77 H. J. Fell, E. J. Samuelson, M. R. Andersson, J. Als-Nielsen, G. Grübel and J. Mardalen, *Synth. Met.*, 1995, **73**, 279.
- 78 K. E. Aasmundtvei, E. J. Samuelson, W. Mammo, M. Svensson, M. R. Andersson, L. A. A. Pettersson and O. Inganäs, *Macromolecules*, 2000, **33**, 5481.
- 79 M. R. Andersson, O. Thomas, W. Manno, M. Svensson, M. Theander and O. Inganäs, *J. Mater. Chem.*, 1999, **9**, 1933.
- 80 C. J. Brabec, C. Winder, M. C. Scharber, N. S. Sariciftci, J. C. Hummelen, M. Svensson and M. R. Andersson, *J. Chem. Phys.*, 2001, **15**, 7235.
- 81 C. J. Brabec, C. Winder, M. Scharber, N. S. Sariciftci, M. R. Andersson, O. Inganäs and J. C. Hummelen, *Mater. Res. Symp. Proc.*, 2000, **598**, B 3.24.1-6.
- 82 X. Wei, Z. V. Vardeny, N. S. Sariciftci and A. J. Heeger, *Phys. Rev. B*, 1996, **53**, 2187.
- 83 R. Österbacka, C. P. An, X. M. Jiang and Z. V. Vardeny, *Science*, 2000, **287**, 839.
- 84 D. Beljonne, J. Cornil, H. Sirringhaus, P. J. Brown, M. Shkunov, R. H. Friend and J. L. Bredas, *Adv. Funct. Mater.*, 2001, **11**, 229.
- 85 L. S. Roman, W. Manno, L. A. A. Pettersson, M. R. Andersson and O. Inganäs, *Adv. Mater.*, 1998, **10**, 774.
- 86 U. Scherf and E. W. List, *Adv. Mater.*, 2002, **14**, 477.
- 87 A. Charas, J. Morgado, J. M. G. Martinho, L. Alcacer, S. F. Lim, R. H. Friend and F. Cacialli, *Polymer*, 2003, **44**, 1843.
- 88 R. Pacios and D. D. C. Bradley, *Synth. Met.*, 2002, **127**, 261.
- 89 M. Svensson, F. Zhang, S. C. Veenstra, W. J. H. Verhees, J. C. Hummelen, J. M. Kroon, O. Inganaes and M. R. Andersson, *Adv. Mater.*, 2003, **15**, 988.
- 90 A. Dhanabalan, P. A. van Hal, J. K. J. van Duren and R. A. J. Janssen, *Synth. Met.*, 2001, **121**, 2175.
- 91 A. Dhanabalan, J. K. J. van Duren, P. A. Van Hal, J. L. J. van Dongen and R. A. J. Janssen, *Adv. Funct. Mater.*, 2001, **11**, 255.
- 92 D. Muehlbacher, H. Neugebauer, A. Cravino, N. S. Sariciftci, J. K. J. van Duren, A. Dhanabalan, P. van Hal, R. A. J. Janssen and J. K. Hummelen, *Mol. Cryst. Liq. Cryst.*, 2002, **385**, 85.
- 93 J. K. J. van Duren, A. Dhanabalan, P. A. van Hal and R. A. J. Janssen, *Synth. Met.*, 2001, **121**, 1587.
- 94 C. J. Brabec, C. Winder, N. S. Sariciftci, H. C. Hummelen, A. Dhanabalan, P. A. van Hal and R. A. J. Janssen, *Adv. Funct. Mater.*, 2002, **12**, 709.
- 95 C. Winder, G. Matt, J. C. Hummelen, R. A. J. Janssen, N. S. Sariciftci and C. J. Brabec, *Thin Solid Films*, 2002, **403-404**, 373.
- 96 G. Yu, H. Nishino, A. J. Heeger, T. A. Chen and R. D. Rieke, *Synth. Met.*, 1995, **72**, 249.
- 97 S. Tasch, E. J. W. List, C. Hochfilzer, G. Leising, P. Schlichting, U. Rohr, Y. Geerts, U. Scherf and K. Müllen, *Phys. Rev. B*, 1997, **56**, 4479.
- 98 B. Hu, N. Zhang and F. E. Karasz, *J. Appl. Phys.*, 1998, **83**, 6002.
- 99 P. Peumans, A. Yakimov and S. R. Forrest, *J. Appl. Phys.*, 2003, **93**, 3693.
- 100 L. Sicot, B. Geffroy, A. Lorin, P. Raimond, C. Sentein and J. M. Nunzi, *J. Appl. Phys.*, 2001, **90**, 1047.
- 101 S. S. Pandey, K. Rikitake, W. Takashima and K. Kaneto, *Curr. Appl. Phys.*, 2003, **3**, 107.
- 102 D. Kuciauskas, S. Linz, G. R. Seely, A. L. Moore, T. A. Moore, D. Gust, T. Drovetskaya, C. A. Reed and P. D. W. Boyd, *J. Phys. Chem.*, 1996, **100**, 15926.
- 103 E. Peeters, P. A. van Hal, J. Knool, C. J. Brabec, N. S. Sariciftci, J. C. Hummelen and R. A. J. Janssen, *J. Phys. Chem. B*, 2000, **104**, 10174.
- 104 M. A. Loi, P. Denk, H. Hoppe, H. Neugebauer, C. Winder, D. Meissner, C. J. Brabec, N. S. Sariciftci, A. Gouloumis, P. Vazquez and T. Torres, *J. Mater. Chem.*, 2003, **13**, 700.
- 105 L. Chen, L. S. Roman, D. M. Johanson, M. Svensson, M. R. Andersson, R. A. J. Janssen and O. Inganaes, *Adv. Mater.*, 2000, **12**, 1110.
- 106 H. Hiramoto, M. Suezaki and M. Yokoyama, *Chem. Lett.*, 1990, **3**, 327.
- 107 A. Yakimov and S. Forrest, *Appl. Phys. Lett.*, 2002, **80**, 1667.
- 108 M. Niggemann, B. Bläsi, A. Gombert, A. Hinsch, H. Hoppe, P. Lalanne, D. Meissner and V. Wittwer, *Proceedings of the 17th European Photovoltaic Solar Energy Conference*, 2001.
- 109 L. S. Roman, O. Inganaes, T. Granlund, T. Nyberg, M. Svensson, M. R. Andersson and J. C. Hummelen, *Adv. Mater.*, 2000, **12**, 189.
- 110 W. U. Huynh, J. J. Dittmer and A. P. Alivisatos, *Science*, 2002, **295**, 2425.
- 111 J. Krueger, R. Plass, M. Graetzel and H. J. Matthieu, *Appl. Phys. Lett.*, 2002, **81**, 367.